Investigation of the ankle contact forces in a foot with hammer toe: A comparison of patient-specific results from finite element modeling and musculoskeletal simulation

M. Moayedi, R. Naemi, A. R. Arshi, M. Akrami, M. Salehi

Abstract— **The internal forces and stresses in the tissue are important as they are linked to the risk of mechanical trauma and injuries. Despite their value, the internal stresses and forces cannot be directly measured in-vivo. A previously validated 3D finite element model (FEM) was constructed using Magnetic Resonance Imaging (MRI) of a person with diabetes and hammer toe deformity. The foot model simulated at five different instances during the stance phase of gait. The internal stress distribution on the talus that was obtained using the FEM simulation, was used to calculate the joint reaction force at the ankle joint. In addition, the musculoskeletal model (MSM) of the participant with hammer toe foot was developed based on the gait analysis and was used to determine the muscle forces and joint reactions. The result showed that the vertical reaction forces obtained from the FEM and MSM follow a similar trend through the stance phase of gait cycle and are significantly correlated (R=0.99). The joint reaction forces obtained through the two methods do not differ for the first 25% of the gait cycle, while the maximum difference was ~0.7 Body weight that was observed at 50% of the stance phase.**

Clinical Relevance: **Finite element modeling and musculoskeletal simulation can shed light on the internal forces in the ankle in pathological conditions such as hammer toe. The similarities and differences observed in the joint reaction forces calculated from the two methods can have implications in assessing the interventions in a clinic.**

I. Introduction

Lower extremity health is an important factor in determining the quality of life, while this is affected by several factors such as age, weight, musculoskeletal problems, physical activity, inappropriate shoes, etc. [1-6]. The joints are commonly the most vulnerable part of the kinematic chain of the human locomotor system. Hence the internal joint forces and moments have been considered in various studies [7-11]. The joint forces have been investigated based on classical force equilibrium equations [12], in vivo values [13, 14], and computational modeling such as musculoskeletal modeling [15, 16]. However, a non-invasive in-vivo assessment of the internal joint forces can only be achieved using modeling and simulation approaches. Despite this there is a scarcity of comparison of predicted joint force results from Finite Element Modeling against the commonly used method of Musculoskeletal simulation. The aim of this study was to investigate the ankle joint force obtained using the two different methods of Finite Element Modeling and Musculoskeletal simulation.

II. Method

A. Gait Analysis

Three-dimensional gait analysis was performed on a male participant with hammer toes deformity in the left foot (age: 53, height: 165 cm, weight:93 Kg) in a lab equipped with 10 infrared motion capture camera system (Vicon, Oxford, UK) with sampling at 100 Hz. The 36 markers, consisting of 24 main and 12 extra markers were placed on the trunk and lower limb based on the plug-in gait method [17-21]. Two force plates (Kistler, Winterthur, Switzerland) were utilized for obtaining the ground reaction forces (GRFs). The participant walked barefoot at a self-selected speed across the walkway. GRFs and markers trajectory for static and several dynamic trials were recorded synchronously using Nexus software (Vicon, Oxford, UK).

B. MSM

For the purpose of predicting the joint reaction forces, the generic musculoskeletal model, 'gait 2392' was deployed using OpenSim software [22]. Static trial data were used for scaling the generic model that was validated in our previous study [23]. Walking movements were reconstructed using inverse kinematic, and muscle forces were predicted with static optimization. At the end of the MSM steps, the joint forces were obtained using the Joint Reaction Analysis in OpenSim. This tool is known as a post-processor, which needs inverse kinematic, and static optimization results (muscle forces) and GRFs as inputs.

III. FEM

The 3D bones and a soft tissue model of the left foot of the participant with hammer toe were segmented and constructed based on MRI medical images using the Mimics software (Materialise, Leuven, Belgium). The MRI of left foot was taken in unloaded condition using a 1.5 T MRI scan (Philips Ingenia, spacing between slices: 0.5 mm and slice thickness: 1 mm, sequence 3D mDion Te Hr, TE/TR 9/29) which the 90° angle between leg and foot was maintained by pads and

M. Moayedi is with Department of Mechanical Engineering, Amirkabir University of Technology, Iran (e-mail: M.moayedi@ aut.ac.ir).

M. Salehi, is with Department of Mechanical Engineering, Amirkabir University of Technology, Iran (e-mail: Msalehi@ aut.ac.ir).

A. R. Arshi is with Biomechanics and Sports Engineering Groups, Biomedical Engineering Department, Amirkabir University of Technology, Iran (e-mail: arshi@aut.ac.ir).

M. Akrami is with Department of Engineering, College of Engineering, Mathematics, and Physical Sciences, University of Exeter, UK (e-mail: M.Akrami@exeter.ac.uk).

R. Naemi is with Centre for Biomechanics and Rehabilitation Technologies, Staffordshire University, UK (corresponding author; phone: +44 (0) 1782 295879; e-mail: naemi@staffs.ac.uk).

pillows. The parts of the model were: 30 bones (14 phalanges, medial and lateral sesamoids, 5 metatarsals, cuboid, 3 cuneiforms, navicular, calcaneus, talus, and the distal parts of the tibia and fibula) and the bulk of soft tissue; to growth the precision of the model, 74 cartilage layers were added to the model as 37 pairs of joints between bones. The interaction among cartilage layers was considered as surface-to-surface frictionless contact.

All the parts (the cartilage parts, one Achilles tendon, 30 bones, and bulk of soft tissue) were imported to ABAQUS software (SIMULIA, Providence, USA) to carry out the finite element analysis. Achilles tendon attached and tied over the calcaneus and also, since the ligaments are not well defined in MRI images, a total of 2174 truss elements were added to the model to indicate major ligaments and the plantar fascia inserted based on anatomical atlases [24] (see Fig. 1). All the ligaments, cartilages, bones, and Achilles tendon were embedded in the bulk of soft tissue that enclosed all the other parts. A 3D rigid rectangular part was added to the model as the ground. Contact between plantar of soft tissue and plate was considered surface to surface with 0.6 frictional coefficient mentioned in the earlier study [25]. Material properties of all components were considered homogeneous and isotropic from the literature [26,27] (see table 1).

A. Walking simulation

Five instants (heel strike (5%), early stance (25%), mid-stance (50%), late stance (75%), and toe-off (90%)) of a stance phase during the gait cycle were carried out under quasi-static analysis. At each instant, the GRFs and muscle forces associated with each event were added to the model. The upper surface of the soft tissue, distal fibula, and tibia was fixed during the analysis. GRFs recorded in the gait trials were induced to the ground plate at COP. COP's location was determined in accordance with the relative location of COP and anatomical landmarks. To induce the effect of major muscles, the six considered muscle force vectors consisting of the soleus, medial and lateral gastrocnemius were applied to the Achilles tendon, and also the force of tibialis anterior, tibialis posterior, and peroneus longus were assigned to their respective bones along the muscle force vectors specified using the OpenSim model[28, 29].

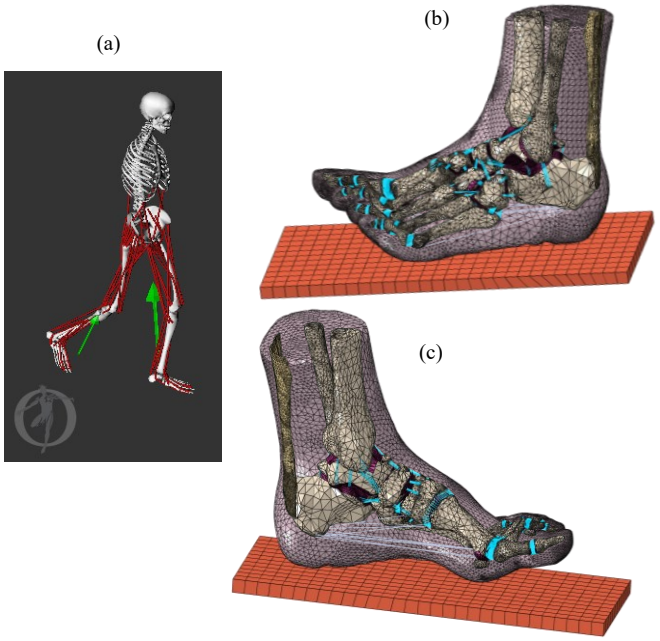

Figure 1. Opensim and ABAQUS model (a) MSM (b) lateral view of FEM (c) medial view of FEM

IV. RESULTS

Hence for comparing the predicted joint force by two methods, vertical force reaction in the ankle on talus was considered. Stresses distribution in the vertical direction at five different events of stance phase are shown in Fig. 2. To calculate the induced vertical force on the talus, stress amplitude in the vertical direction was multiplied by objected contact area on the ankle joint (surface of talus which is in contact with tibia and fibula) on the surface with the vertical normal vector. For finding the percentage of each area with the same color of stress contour, Image analysis was performed with open-source ImageJ software.

The average value of each stress color spectrum was placed in force calculation. The grey color in Fig. 2 shows tension stresses, and as the purpose is to find contact force and this kind of force makes compression stresses, these grey areas were ignored in the calculation. The ankle vertical joint force during the stance phase normalized by body weight is shown in Fig. 3.

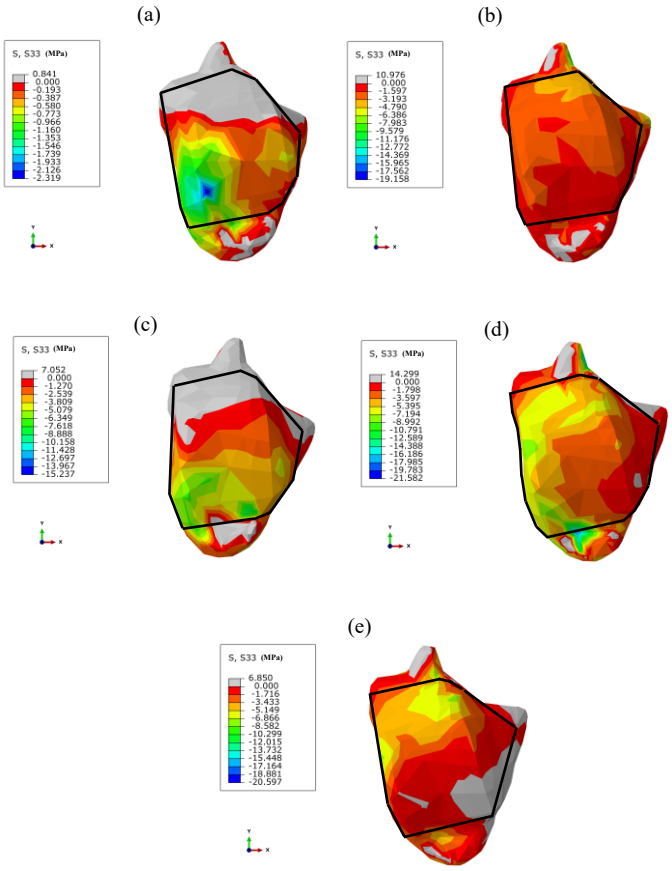

Figure 2. Stress distribution on talus from top view. (a) heel strike (b) early stance (c) mid-stance (d) late stance (e) toe-off. The approximate contact area at the ankle joint on the talus is specified using the black line.

TABLE I. ELEMENT TYPES AND MATERIAL PROPERTIES [26, 27] USED IN FEM

Components	Young's modulus (MPa)	Poisson's ratio	Cross section (mm^2)	Element Type
Hard tissue (bones)	7300	0.3	--	Tetrahedral
Ligament	260	--	18.4	Truss
Cartilage	1	0.4	--	Tetrahedral
Plantar fascia	350	--	290.7	Truss
Ground support	17000	0.1	--	Linear hexahedral
Achilles tendon	816	3.0	--	Tetrahedral
Encapsulated soft tissue	Hyperelastic (second-order polynomial strain energy potential equation, C_{10} = 0.08556 Nmm^{-2},C_{01} = -0.05841 Nmm^{-2}, C_{20} = 0.03900 Nmm^{-2}, C_{11} = -0.02319 Nmm^{-2}, C_{02} = 0.00851 Nmm^{-2},D_1 = 3.65273 mm^2N^{-1}, D_2 = 0.0000 mm^2N^{-1})			Tetrahedral

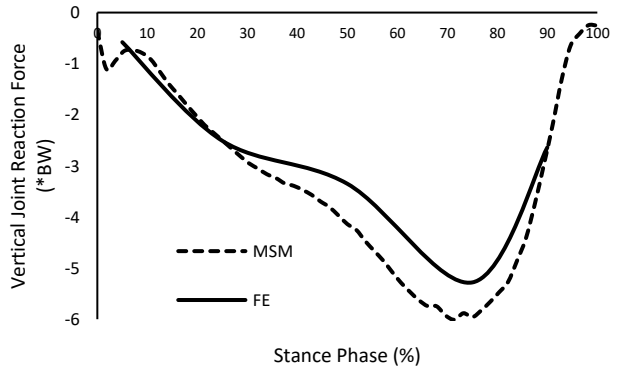

Figure 3. Predicted vertical ankle reaction force by MSM and FEM

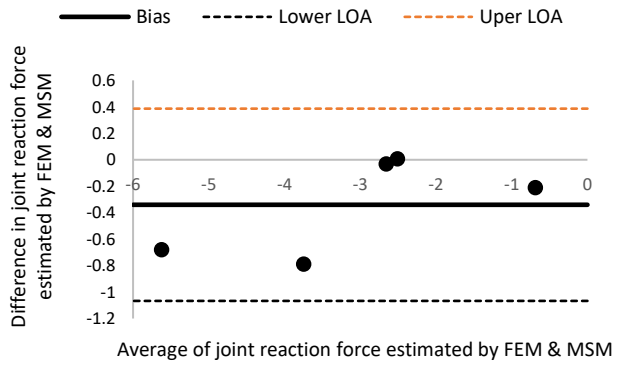

Figure 4. Bland-Altman analysis for predicted ankle force by MSM and FEM

V. CONCLUSION

Pearson correlation coefficient for predicted vertical ankle reaction force by MSM and FEM is equal to 0.99. Therefore, it can be said that the graph of ankle force changes resulted from two different methods have a similar pattern which indicates that there is a considerable correlation between the two methods. As shown in fig. 4 Bland-Altman analysis chart, the difference between the results of the two methods lie along upper and lower LOA lines which indicates the agreement between the two methods. The root-mean-square deviation (RMSD) of the results is equal to 0.59.

Previous studies showed the FEM [30, 31] and MSM [32, 33] separately are useful in the biomechanical analysis, and also it is mentioned that using the MSM results in the FEM, make more accurate results [28,29,34]. This study shows that these two methods, in addition to being an appropriate complement to each other, can also be a way to validate one other. In other words, as shown in Fig 2, it can be possible to find the distribution of the internal load and stresses of the body by FEM, which has become more accurate as well as validated with the help of MSM. These results show that FEM is a reliable tool for predicting the internal body forces, especially joint reaction forces, which have received less attention.

The result showed that the vertical reaction forces obtained from the FEM and MSM follow a similar trend through the stance phase of gait cycle are significantly correlated (R=0.99). The forces do not differ for the first 25% of the gait cycle. The maximum difference observed was ~0.7 Body weight at 50% of the stance phase.

One of the possible sources of this discrepancy could be the differences that may arise as a result of static rather than a dynamic solution of the foot model. In addition, the areas on talus for which a small tensile stress are observed could have decreased the average normal compressive force on the talus surface. Future studies need to look at the source of this difference in light of further validations in cadaveric models.

REFERENCES

[1] D. R. Bonanno, K. B. Landorf, S. E. Munteanu, G. S. Murley, and H. B. Menz, "Effectiveness of foot orthoses and shock-absorbing insoles for the prevention of injury: a systematic review and meta-analysis," British journal of sports medicine, vol. 51, pp. 86-96, 2017.

[2] D. Murphy, D. Connolly, and B. Beynnon, "Risk factors for lower extremity injury: a review of the literature," British journal of sports medicine, vol. 37, pp. 13-29, 2003.

[3] B. S. Neal, I. B. Griffiths, G. J. Dowling, G. S. Murley, S. E. Munteanu, M. M. F. Smith, et al., "Foot posture as a risk factor for lower limb overuse injury: a systematic review and meta-analysis," Journal of foot and ankle research, vol. 7, pp. 1-13, 2014.

[4] F. G. Neely, "Intrinsic risk factors for exercise-related lower limb injuries," *Sports medicine,* vol. 26, pp. 253-263, 1998.

[5] A. K. Wills, Gait kinematics and risk factors for overuse anterior knee pain: University of Surrey (United Kingdom), 2006.

[6] D. L. López, L. C. González, M. E. L. Iglesias, J. L. S. Canosa, D. R. Sanz, C. C. Lobo, et al., "Quality of life impact related to foot health in a sample of older people with hallux valgus," Aging and disease, vol. 7, p. 45, 2016.

[7] C. R. Winby, D. G. Lloyd, T. F. Besier, and T. B. Kirk, "Muscle and external load contribution to knee joint contact loads during normal gait," *Journal of biomechanics,* vol. 42, pp. 2294-2300, 2009.4

[8] G. Valente, L. Pitto, D. Testi, A. Seth, S. L. Delp, R. Stagni, *et al.*, "Are subject-specific musculoskeletal models robust to the uncertainties in parameter identification?," *PLoS One,* vol. 9, p. e112625, 2014.

[9] A. Karatsidis, M. Jung, H. M. Schepers, G. Bellusci, M. de Zee, P. H. Veltink, *et al.*, "Predicting kinetics using musculoskeletal modeling and inertial motion capture," *arXiv preprint arXiv:1801.01668,* 2018.

[10] R. L. Thompson, J. K. Gardner, S. Zhang, and J. A. Reinbolt, "Lower-limb joint reaction forces and moments during modified cycling in

healthy controls and individuals with knee osteoarthritis," *Clinical Biomechanics,* vol. 71, pp. 167-175, 2020.

[11] K. M. Steele, M. S. DeMers, M. H. Schwartz, and S. L. Delp, "Compressive tibiofemoral force during crouch gait," *Gait & posture,* vol. 35, pp. 556-560, 2012.

[12] P. Procter and J. Paul, "Ankle joint biomechanics," *Journal of biomechanics,* vol. 15, pp. 627-634, 1982.

[13] H. J. Kim, J. W. Fernandez, M. Akbarshahi, J. P. Walter, B. J. Fregly, and M. G. Pandy, "Evaluation of predicted knee-joint muscle forces during gait using an instrumented knee implant," *Journal of orthopaedic research,* vol. 27, pp. 1326-1331, 2009.

[14] A. Zargham, M. Afschrift, J. De Schutter, I. Jonkers, and F. De Groote, "Inverse dynamic estimates of muscle recruitment and joint contact forces are more realistic when minimizing muscle activity rather than metabolic energy or contact forces," *Gait & posture,* vol. 74, pp. 223-230, 2019.

[15] B. A. Knarr and J. S. Higginson, "Practical approach to subject-specific estimation of knee joint contact force," *Journal of biomechanics,* vol. 48, pp. 2897-2902, 2015.

[16] T. L.-W. Chen, Y. Wang, D. W.-C. Wong, W.-K. Lam, and M. Zhang, "Joint contact force and movement deceleration among badminton forward lunges: a musculoskeletal modelling study," *Sports Biomechanics,* pp. 1-13, 2020.

[17] Docs.vicon.com, PDF Downloads for Vicon Nexus - Nexus 2.11 Documentation -Vicon Documentation [online] Available at: https://docs.vicon.com/display/Nexus211/PDF+downloads+for+Vicon+Nexus, 2021. (Accessed 14 January 2021).

[18] F. Stief, H. Böhm, K. Michel, A. Schwirtz, and L. Döderlein, "Reliability and accuracy in three-dimensional gait analysis: a comparison of two lower body protocols," *Journal of applied biomechanics,* vol. 29, pp. 105-111, 2013.

[19] P. J. Renaud, *Three-dimensional kinematics of the lower limbs during ice hockey skating starts on the ice surface*: McGill University (Canada), 2016.

[20] E. Flux, M. van der Krogt, P. Cappa, M. Petrarca, K. Desloovere, and J. Harlaar, "The Human Body Model versus conventional gait models for kinematic gait analysis in children with cerebral palsy," *Human movement science,* vol. 70, p. 102585, 2020.

[21] A. Leardini, M. G. Benedetti, L. Berti, D. Bettinelli, R. Nativo, and S. Giannini, "Rear-foot, mid-foot and fore-foot motion during the stance phase of gait," *Gait & posture,* vol. 25, pp. 453-462, 2007.

[22] S.L. Delp, F.C. Anderson, A.S. Arnold, P. Loan, A. Habib, C.T. John, E. Guendelman, D.G. Thelen, OpenSim: open-source software to create and analyze dynamic simulations of movement, IEEE Trans. Biomed. Eng. 54 (11) (Oct. 2007) 1940–1950,

[23] M. Moayedi, A. Arshi, M. Salehi, M. Akrami, and R. Naemi, "Associations between changes in loading pattern, deformity, and internal stresses at the foot with hammer toe during walking; a finite element approach," *Computers in Biology and Medicine,* vol. 135, p. 104598, 2021.

[24] R. Drake, A. W. Vogl, A. W. Mitchell, R. Tibbitts, and P. Richardson, *Gray's Atlas of Anatomy E-Book*: Elsevier Health Sciences, 2020.

[25] M. Zhang and A. Mak, "In vivo friction properties of human skin," *Prosthetics and orthotics International,* vol. 23, pp. 135-141, 1999.

[26] J. T.-M. Cheung, M. Zhang, A. K.-L. Leung, and Y.-B. Fan, "Three-dimensional finite element analysis of the foot during standing—a material sensitivity study," *Journal of biomechanics,* vol. 38, pp. 1045-1054, 2005.

[27] C. Mkandawire, W. R. Ledoux, B. J. Sangeorzan, and R. P. Ching, "Foot and ankle ligament morphometry," *Journal of Rehabilitation Research & Development,* vol. 42, 2005.

[28] M. Akrami, Z. Qian, Z. Zou, D. Howard, C. J. Nester, and L. Ren, "Subject-specific finite element modelling of the human foot complex during walking: sensitivity analysis of material properties, boundary and loading conditions," *Biomechanics and modeling in mechanobiology,* vol. 17, pp. 559-576, 2018.

[29] Z.-h. Qian, L. Ren, L.-q. Ren, and A. Boonpratatong, "A three-dimensional finite element musculoskeletal model of the human foot complex," in *6th World Congress of Biomechanics (WCB 2010). August 1-6, 2010 Singapore*, 2010, pp. 297-300.

[30] Z. Wang, et al. A finite element model of flatfoot (pes planus) for improving surgical plan in Engineering in Medicine and Biology Society (EMBC), 2014 36th Annual International Conference of the IEEE. 2014.

[31] E. Brilakis, et al., Effects of foot posture on fifth metatarsal fracture healing: a finite element study. The Journal of Foot and Ankle Surgery, 2012. 51(6): p. 720-728

[32] A. Rajagopal, C. L. Dembia, M. S. DeMers, D. D. Delp, J. L. Hicks, and S. L. Delp, "Full-body musculoskeletal model for muscle-driven simulation of human gait," *IEEE transactions on biomedical engineering,* vol. 63, pp. 2068-2079, 2016

[33] E. S. Arch, S. J. Stanhope, and J. S. Higginson, "Passive-dynamic ankle–foot orthosis replicates soleus but not gastrocnemius muscle function during stance in gait: insights for orthosis prescription," *Prosthetics and orthotics international,* vol. 40, pp. 606-616, 2016.

[34] A. Scarton, A. Guiotto, T. Malaquias, F. Spolaor, G. Sinigaglia, C. Cobelli*, et al.*, "A methodological framework for detecting ulcers' risk in diabetic foot subjects by combining gait analysis, a new musculoskeletal foot model and a foot finite element model," *Gait & posture,* vol. 60, pp. 279-285, 2018.